

Charge transport in transparent single-wall carbon nanotube networks

This article has been downloaded from IOPscience. Please scroll down to see the full text article.

2007 J. Phys.: Condens. Matter 19 446006

(<http://iopscience.iop.org/0953-8984/19/44/446006>)

View [the table of contents for this issue](#), or go to the [journal homepage](#) for more

Download details:

IP Address: 129.252.86.83

The article was downloaded on 29/05/2010 at 06:29

Please note that [terms and conditions apply](#).

Charge transport in transparent single-wall carbon nanotube networks

Manu Jaiswal¹, Wei Wang², K A Shiral Fernando², Ya-Ping Sun² and Reghu Menon¹

¹ Department of Physics, Indian Institute of Science, Bangalore 560012, India

² Department of Chemistry and Laboratory for Emerging Materials and Technology, Clemson University, Clemson, SC 29634-0973, USA

E-mail: manu@physics.iisc.ernet.in

Received 15 July 2007, in final form 23 August 2007

Published 24 September 2007

Online at stacks.iop.org/JPhysCM/19/446006

Abstract

We report the electric-field effects and magnetotransport in transparent networks of single-wall carbon nanotubes (SWNT). The temperature dependence of conductance of the network indicates a 2D Mott variable-range hopping (VRH) transport mechanism. Electric field and temperature are shown to have similar effects on the carrier hops and identical exponents for the conductance of the network are obtained from the high electric field and temperature dependences. A power-law temperature dependence with an exponent $3/2$ for the threshold field is obtained and explained as a result of the competing contributions from electric field and phonons to the carrier hop. A negative magnetoresistance (MR) is observed at low temperatures, which arises from a forward interference scattering mechanism in the weak scattering limit, consistent with the VRH transport.

(Some figures in this article are in colour only in the electronic version)

1. Introduction

The charge transport in single-wall carbon nanotube (SWNT) systems can vary from diffusive to ballistic, depending upon the extent and nature of disorder. Although high quality individual SWNT often show ballistic transport, as disorder increases variable-range hopping (VRH) conduction is widely observed [1–3]. A comparison of the roles played by temperature and electric field can throw light onto the nature of hopping transport. Such an investigation is particularly interesting for carbon nanotube systems because the nature of localization is non-trivial due to the presence of extended wavefunctions along the individual tube (or bundle of tubes). While electric field is predicted to play a role identical to that of temperature for hopping transport in amorphous and doped crystalline semiconductors, similar investigations

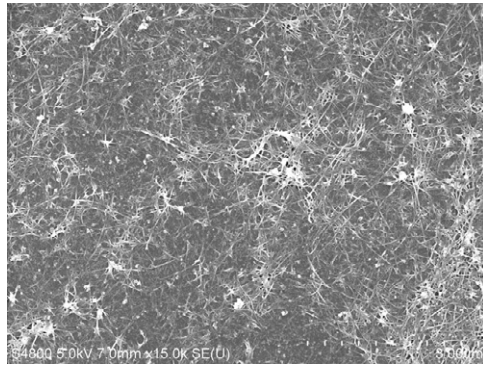


Figure 1. SEM image of the transparent SWNT network (scale bar is 3 μm).

are required in nanotube systems in order to understand the hopping process in which both dimensionality and disorder play important roles [4]. The effects of magnetic field at low temperatures also offer intriguing physics for SWNT systems and can provide further insight into the nature of scattering processes for the carriers undergoing hops [5].

In this paper, the low-temperature electric and magnetic field effects are reported on optically transparent networks of SWNTs. The recent interest generated in these novel materials originates not only from the interesting physics they offer but also from their potential applications as transparent flexible electrodes and transistors in organic nanoelectronics [6]. The transparencies of these networks are already comparable to those of conventional transparent electrodes, indium–tin oxide, and an understanding of the transport phenomenon is essential towards making them viable alternatives to the latter. Hopping transport has been recently reported in these networks, with metallic fraction of tubes playing an important role in conduction [1]. In the present work, we report on various aspects of charge transport in transparent SWNT networks including the dependence of network conductance on temperature, electric and magnetic fields at low temperatures, towards evolving a consistent picture for transport.

2. Experimental details

The SWNTs were prepared by the carbon-arc method and comprised of metallic and semiconducting tubes in the ratio of 1:2 (i.e. 33% of the tubes are metallic). The nanotubes were dispersed in dimethylformamide (DMF) via homogenization followed by sonication for 60 min. The dispersion solution was sprayed onto a heated glass-slide held at 150 °C [7]. The SWNTs are randomly oriented in an interconnected network with high optical transparency (>85% at 550 nm wavelength) and a scanning electron microscope (SEM) image of the network is shown in figure 1. The SWNTs have a bundle diameter of 10–20 nm and an average length of over 1 μm .

The pulsed voltage–current (V – I) and magnetic field measurements were performed in a Janis variable-temperature cryogenic system equipped with an 11 T superconducting magnet. The sample is immersed directly in a vapour or liquid helium bath. This together with the fact that the nanotube network is dilute (i.e. packing fraction is low 20–25%) ensures good thermal contact between the entire network and the bath. The contact geometry used in the measurements was the conventional ‘collinear’ four-probe type with a contact separation of 1 mm, such that an ‘average’ network property was measured. The nonlinear V – I

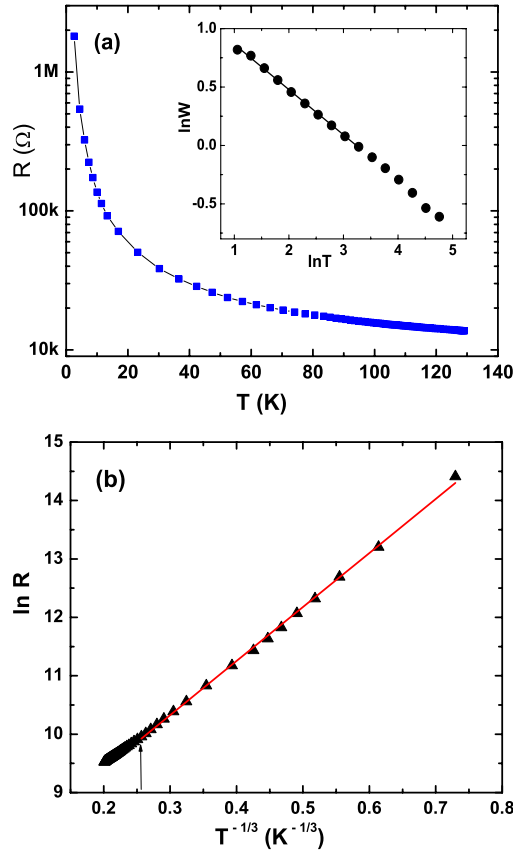


Figure 2. (a) R versus T . Inset: reduced activation energy W versus T with linear fit. (b) $\ln R$ versus $T^{-1/3}$ showing the linear relationship.

characteristics of the system were obtained using a pulsed four-probe technique: a short voltage pulse (<10 ms) was applied across the outer contacts of the sample using a programmable pulsed voltage source (model Keithley-2400) and the current measured through it. Additionally, the voltage drop was measured between the inner contacts after a delay (minimum 3 ms) from the time of application of voltage bias using an electrometer (model Keithley-6517) synchronized with the source. This delay is introduced to ensure that the voltage at the sample has reached its full level before a measurement is performed. For the temperature and magnetic-field dependence of four-probe network resistance, a small current was applied (typically $I < 0.2 \mu A$) to limit the heat dissipation as well as to have a low bias appearing across the sample.

3. Results and discussion

Measurements were performed on samples showing optical transparency of 85–90% at 550 nm wavelength and the typical results are presented below. Our network shows hopping transport (figure 2(a)) with a resistivity ratio, $R_{4.2}/R_{300} \sim 50$; and the exponent for hopping conduction is found by evaluating the reduced activation energy $W(T) = -\partial \ln R(T)/\partial \ln T$ as shown in the inset of figure 2(a). The graph yields an exponent of 0.38, close to $1/3$ as seen from the

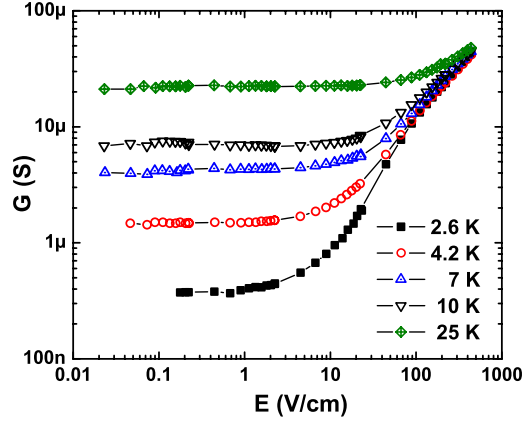


Figure 3. Electric-field dependence of network conductance at various low temperatures.

negative slope of the W -plot. This value favours a 2D Mott VRH conduction for the network described by the equation for conductance [8]:

$$G(T) = G_{0T} \exp[-(T_0/T)^p] \quad (1)$$

where $p = 0.38 \sim 1/3$, G_{0T} is characteristic of the sample, $k_B T_0 = 3/\lambda^2 N(0)d$, λ is the localization length, $N(0)$ is the density of states (DOS) at the Fermi level and d is the sample thickness. Note that the metallic DOS at the Fermi level should be rescaled to account for the volume packing-fraction of tubes [9]. Disorder is present along the individual nanotubes or along tube and bundle boundaries, and both are relevant to the hopping transport. The value of $T_0 = 292$ K is obtained from the W -plot, $\ln W = -p \ln T + \ln(pT_0^p)$, and an estimate of localization length can be obtained using (1), $\lambda \sim 9$ nm. This value can be correlated to the typical size of nanotube-bundles [9]. Figure 2(b) shows the linear relationship between $\ln R$ and $T^{-1/3}$.

The conductance of the network, $G = J/E$, is plotted as a function of applied pulsed electric field in figure 3. The conductance is nearly constant at low electric fields, especially at higher temperatures, and it increases at higher fields till it becomes nearly temperature-independent. At lower temperatures ($T < 4.2$ K) the conductance increases by nearly two orders of magnitude for $E \sim 500$ V cm $^{-1}$. Non-ohmic conductivity of the type seen in our system can result from a redistribution of carrier energy under the effect of electric field [9]. For hopping conduction the field dependence was shown to be $I = I_0 \exp[-(E_0/E)^v]$, with E_0 being a characteristic constant of the system [4]. However, the electric-field dependence is better described by an equation more similar to (1) [10–12]:

$$G(E) = G_{0E} \exp[-(E_0/E)^\Delta]. \quad (2)$$

These equations are strictly valid in the limit of $T \rightarrow 0$ K. Our analysis shows that for our network the conductance-expression (2) is a more appropriate description for the electric-field dependence than the current-expression. To analyse the field-dependence, we calculate the field scaling function, $\beta_E = -\partial \ln G / \partial \ln E = \Delta(\ln G - \ln G_{0E})$ for the lowest temperatures [10]. The field scaling function together with the temperature scaling function $\beta_T = -\partial \ln G / \partial \ln T = p(\ln G - \ln G_{0T})$ is plotted as a function of $\ln G$ in figure 4(a) [13]. The value of exponent Δ obtained is $0.36 \sim 1/3$ at the lowest temperature, virtually identical to the temperature exponent. Indeed we find that the slope of β_E (at high field) is nearly the same as the slope of β_T . This result suggests that strong electric field plays a role similar

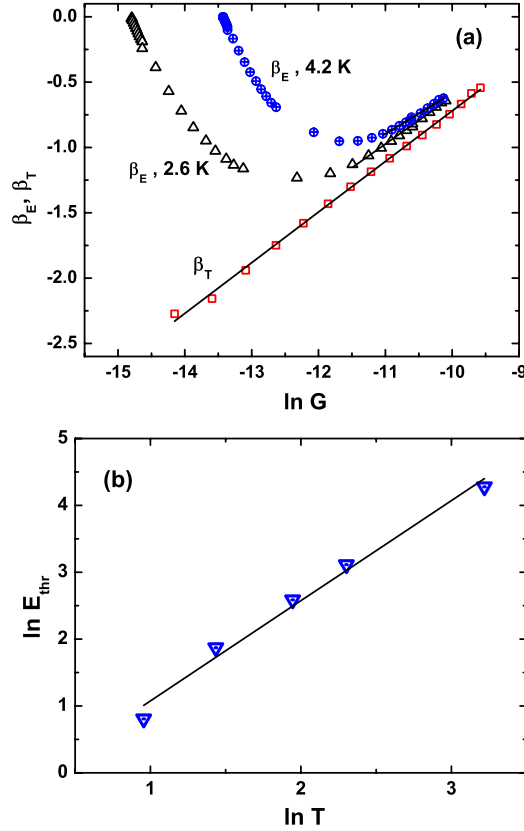


Figure 4. (a) β_T versus $\ln G$ from 2.6 to 140 K. β_E versus $\ln G$ at 2.6 and 4.2 K. Solid lines are fits to regions where a single parameter dominates: $p = 0.38$; $\Delta = 0.36$ at 2.6 K, 0.31 at 4.2 K. (b) $\ln E_{\text{thr}}$ versus $\ln T$. Solid line fit gives the power-law exponent $\sim 3/2$ (error margin is 7%).

to temperature for the low-temperature hopping transport in our network. The applied field modifies the energy of hop between two states by an amount $eER \cos \theta$ where R is the separation of the two states, e is the electronic charge and θ is the angle between field and direction of hop. At high fields for hops in the field direction, electrons can hop without thermal activation by phonons when $eER > W$, where W is the thermal hopping energy [12]. Note that the slope of β_E versus $\ln G$ is negative at higher temperatures and lower fields. Therefore the assumption of single parameter scaling (with electric field alone) is not completely valid for $T > 0$ and only holds at high fields. Additionally we note that the value of G_{0E} ($246 \mu\text{S}$ from 2.6 K data) is close to the value of G_{0T} ($296 \mu\text{S}$), further supporting the identical effects of field and temperature in the limits of low temperature and low bias respectively.

The G - E plot in figure 3 suggest the presence of a threshold field above which the response is non-ohmic. We define a threshold field (E_{thr}) for the field response as the value of electric field for which $\Delta G/G(0) \sim 0.2$, where $G(0)$ is the field-independent conductance in the low-field regime. An empirical relation $E_{\text{thr}} = 0.65T^{3/2}$ is obtained from the slope of the double logarithmic plot of E_{thr} versus T in figure 4(b). The exponent of E_{thr} does not significantly depend upon the precise way the threshold field is defined; for e.g. $\Delta G/G(0) \sim 0.5$ yields a slope of $1.6 \sim 3/2$. The threshold field increases with temperature, since higher fields are required to overcome the contribution from phonons. Above E_{thr} , the carriers start to gain

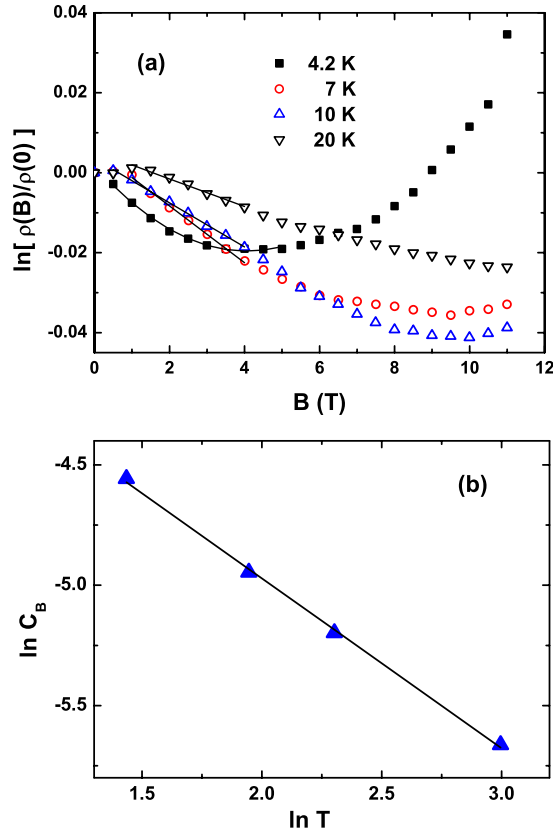


Figure 5. (a) MR versus B at various temperatures. Solid lines are fits described in the text. (b) Temperature dependence of the coefficient of negative-MR.

more of their energy from the electric field than from thermal excitations, until finally the transport becomes activationless at high fields. For 2D Mott VRH, the optimum hopping distance $R \sim T^{-1/3}$ and the average hopping energy $W \sim R^{-2}$, so a simple calculation suggests that the dependence of E_{thr} on temperature will be linear, our exponent is somewhat higher, possibly because the above description holds strictly only at zero bias [12]. We also observe that the quantity $eER/W \approx O(1)$ when $E = E_{\text{thr}}$. It is further seen that this empirical relation is nearly independent of applied transverse magnetic fields up to 11 T and it is therefore intrinsic to the role of electric field in hopping conduction and not dependent on the scattering and interference process associated with magnetic field, as described below.

A negative magnetoresistance (MR) was observed for the network at low temperatures as shown in figure 5(a). For systems close to the metal-insulator transition, the negative MR is often inferred from the suppression of quantum corrections to the conductivity, under magnetic field, i.e. negative MR in weak localization. The interpretation must, however, be consistent with the nature of charge transport. In our disordered network, the temperature and electric-field data support VRH conduction and the magnetotransport must also be analysed within the same framework. A negative MR in the VRH regime has been suggested to arise from a forward interference scattering process. In this model by Nguyen *et al*, the application of a magnetic field removes the destructive interference between multisite hops [14]. The MR is linear with field in the low-/intermediate-field region and linear fits to our data in this region are shown in

figure 5(a). At 4.2 K there is an additional positive contribution from a different mechanism and a term quadratic in field must also be included along with the linear term in order to obtain a satisfactory fit. This quadratic positive contribution most likely arises from the localization originating from wavefunction shrinkage under magnetic field [15]. However, the fits are not fully satisfactory down to zero-field and this minor contribution can be explained due to the complex nature of the scattering process at very low fields [16]. An analytically simpler version of Nguyen's model by Schirmacher considers only a single intermediate hopping site and this model also predicts the temperature dependence of the negative MR in the weak scattering limit, given as [17]:

$$\ln[(\rho(B)/\rho(0))] = -kB/T^s = -C_B B \quad (3)$$

where k is a constant, B is the magnetic field, C_B is the coefficient of magnetic field and s is an exponent close to 1; in the case of strong scattering the MR is expected to be temperature-independent. To evaluate the exponent, the temperature dependence of C_B obtained from the above fits is plotted in figure 5(b) on a double logarithmic scale. The slope gives the exponent $s = 0.71 \pm 0.02$, a value slightly lower than the theoretical prediction.

4. Conclusion

Measurements of the low-temperature electric and magnetic field dependence of conductance in transparent SWNT networks are presented. A 2D Mott VRH is observed for the network and a scaling function analysis shows an identical exponent ($\sim 1/3$) for both high electric field and low temperatures. The charge transport analysis that includes temperature, electric and magnetic field dependences is presented within a consistent framework. Temperature and electric field are shown to play identical roles in the hopping transport. A power-law relation for the temperature dependence of E_{thr} is obtained with an exponent $\sim 3/2$ and is understood to result primarily from the increased contribution of field to the hopping process in comparison to the phonon contribution. A negative MR is observed at low temperatures arising from a forward interference scattering process, and an inverse power-law temperature dependence for this MR suggests a weak scattering process in the system.

Acknowledgments

These measurements were performed at the DST National facility for Low Temperature and High Magnetic Field, Bangalore (we thank Dr V Prasad). MJ thanks CSIR, New Delhi for financial assistance and Y-PS acknowledges financial support from the US National Science Foundation.

References

- [1] Skákalová V, Kaiser A B, Woo Y-S and Roth S 2006 *Phys. Rev. B* **74** 085403
- [2] Vavro J, Kikkawa J M and Fischer J E 2005 *Phys. Rev. B* **71** 155410
- [3] Kim G T, Choi E S, Kim D C, Suh D S, Park Y W, Liu K, Duesberg G and Roth R 1998 *Phys. Rev. B* **58** 16064
- [4] Shklovskii B I 1973 *Sov. Phys.—Semicond.* **6** 1964
- [5] Tarkiainen R, Ahlskog M, Zyuzin A, Hakonen P and Paalanen M 2004 *Phys. Rev. B* **69** 033402
- [6] Grüner G 2006 *J. Mater. Chem.* **16** 3533
- Takenobu T, Takahashi T, Kanbara T, Tsukagoshi K, Aoyagi Y and Iwasa Y 2006 *Appl. Phys. Lett.* **88** 033511
- [7] Li H, Zhou B, Lin Y, Gu L, Wang W, Fernando K A S, Kumar S, Allard L F and Sun Y-P 2004 *J. Am. Chem. Soc.* **126** 1014
- [8] Frydman A and Ovadyahu Z 1995 *Solid State Commun.* **94** 745

-
- [9] Benoit J M, Corraze B and Chauvet O 2002 *Phys. Rev. B* **65** 241405(R)
 - [10] Liu G and Soonpaa H H 1993 *Phys. Rev. B* **48** 5682
 - [11] Licciardello D C and Soonpaa H H 1980 *Surf. Sci.* **98** 225
 - [12] Jana D and Fort J 2004 *Physica B* **344** 62
 - [13] Tremblay F, Pepper M, Newbury R, Ritchie D, Peacock D C, Frost J E F and Jones G A C 1989 *Phys. Rev. B* **40** 3387
 - [14] Nguyen V L, Spivak B Z and Shklovskii B I 1985 *Sov. Phys.—JETP* **62** 1021
 - [15] Shklovskii B I and Efros A L 1984 *Electronic Properties of Doped Semiconductors* (Berlin: Springer)
 - [16] Raikh M E and Wessels G F 1993 *Phys. Rev. B* **47** 15609
 - [17] Schirmacher W 1990 *Phys. Rev. B* **41** 2461